
Helical, Angular and Radial Ordering in Narrow Capillaries

I. ERUKHIMOVICH¹ and A. JOHNER²

¹ *Moscow State University, Moscow 119992 Russia*

² *Institute Charles Sadron, 6 rue Boussingault, 67083 Strasbourg Cedex, France*

PACS **nn.mm.xx** – First pacs description

PACS **nn.mm.xx** – Second pacs description

PACS **nn.mm.xx** – Third pacs description

Abstract. - To enlighten the nature of the order-disorder and order-order transitions in block copolymer melts confined in narrow capillaries we analyze peculiarities of the conventional Landau weak crystallization theory of systems confined to cylindrical geometry. This phenomenological approach provides a quantitative classification of the cylindrical ordered morphologies by expansion of the order parameter spatial distribution into the eigenfunctions of the Laplace operator. The symmetry of the resulting ordered morphologies is shown to strongly depend both on the boundary conditions (wall preference) and dimensionless parameter q_*R , where R is the cylinder radius and q_* is the wave number of the critical order parameter fluctuations, which determine the bulk ordering of the system under consideration. In particular, occurrence of the helical morphologies is a rather general consequence of the imposed cylindrical symmetry for narrow enough capillaries. We discuss also the ODT and OOT involving some other simplest morphologies. The presented results are relevant also to other ordering systems as charge-density waves appearing under addition of an ionic solute to a solvent in its critical region, weakly charged polyelectrolyte solutions in poor solvent, microemulsions etc.

Introduction. – During the last years there has been large interest in the behavior of block copolymer (basically diblock copolymer) melts confined in narrow capillaries, which were studied both experimentally [1–6] and via computer simulation [7–9] as well as by numerical calculations within the self-consistent field theory [1,10,11]. The most characteristic of these morphologies are lamellae ordered normal to the cylinder axis z (slab morphology [10]) and coaxial shells or multiwall morphologies [7,10] as well as various helices [1,8,9], the morphologies' symmetry being strongly depended on the ratio of the gyration radius R_G of the diblock macromolecules under consideration and the radius R of the cylinder the macromolecules are confined to. However, some important issues have not been addressed yet. In particular, the various morphologies (up to 20 in ref [11] and up to 30 in ref [9]) are distinguished only visually by their snapshots and no attempts to relate them to a quantitative order parameter are made until now. Meanwhile, without a quantitative definition of an order parameter and, accordingly, finding the quantitative change of such an order parameter at the phase transitions

one cannot discuss the transitions between the morphologies rigorously. Probably, this is why no accurate phase diagram of the order-disorder and order-order transitions for cylindrically confined block copolymer melts is presented until now. In particular, the phase diagram presented in ref [11] has two important shortcomings: *i*) it is based on a visual distinguishing of the morphologies *only*, and *ii*) the authors assume no modulation of the block copolymer composition along the z -axes, which, obviously, excludes the slab and helical morphologies. Besides, an alternation of some coexisting phases is to occur in cylindrical capillaries already by virtue of the Landau theorem [12] as in any effective 1D system.

Another shortcoming of all the aforementioned studies [1–11] is that they are specifically block copolymer oriented whereas ordering in cylindrically confined systems seems to be much more general. Indeed, the very existence of the various morphologies in block copolymer melts is due to the instability of their homogeneous phase with respect to spatial fluctuations of the polymer concentration with a finite spatial period [13–15]. Thus,

the ODT in block copolymers is only a particular case of the well known weak crystallization instability [16, 17]. The Landau weak crystallization theory (WCT) provides a common physical background for describing such seemingly different physical phenomena as *i*) forming weakly segregated morphologies in molten block copolymers [14], therewith the polymer specific features appear at the stage of the microscopic calculation of the Landau expansion coefficients only, *ii*) appearance of the blue phases in liquid crystals [18, 19], *iii*) charge-density waves generation upon addition of an ionic solute to a solvent in its critical region [20, 21], *iv*) microphase separation in weakly charged polyelectrolyte solutions [22, 23] and *v*) microemulsions [24].

So, the peculiarities found for cylindrically confined block copolymer melts are expected to exist for other nano-ordered systems either and the aim of the present Letter is to present a phenomenological theory of the ordering in narrow capillaries based on the general weak crystallization paradigm.

1. We start with the standard expression for the free energy of the weakly crystallized systems described by a non-uniform scalar order parameter profile $\Phi(\mathbf{r})$, which without any loss of generality could be written as the Landau expansion in powers of Φ up to the 4th order:

$$\frac{vF_{\text{bulk}}}{T} = \int \left(\tau \Phi^2(\mathbf{r}) + ((1 + q_*^{-2} \Delta) \Phi(\mathbf{r}))^2 + \alpha \Phi^3(\mathbf{r}) + \Phi^4(\mathbf{r}) \right) d\mathbf{r}, \quad (1)$$

where v is a constant having dimensionality [l^3] to be defined from microscopic considerations and τ is an effective dimensionless temperature measured from the instability boundary for bulk. In bulk the quadratic term in (1) reads

$$F_{\text{bulk}}^{(2)} = \int \left[\tau + (1 - q^2/q_*^2)^2 \right] |\Phi_{\mathbf{q}}|^2 \frac{d\mathbf{q}}{(2\pi)^3} \quad (2)$$

where $\Phi_{\mathbf{q}} = \int \Phi(\mathbf{r}) \exp(i\mathbf{q}\mathbf{r}) d\mathbf{r}$ is the Fourier component of the order parameter. Obviously, for $\tau > 0$ a minimum (at least, a metastable one) of the free energy (1) is provided for the disordered state ($\Phi(\mathbf{r}) = 0$), whereas for $\tau < 0$ the disordered state is absolutely unstable with respect to the growth of the Fourier components $\Phi_{\mathbf{q}}$ with wave numbers $q = |\mathbf{q}|$ close to the value $q = q_*$. Thus, the parameter $q_*^2 > 0$ characterizes the wave length $L = 2\pi/q_*$ of the critical order parameter fluctuations, which destroy the disordered state in bulk.

The coefficient α appearing in the free energy expression (1) depends on the physical nature of the system. In this paper we restrict ourselves to the case $\alpha = 0$, when the only ordered phase appearing in bulk systems described by (1) is lamellar, and show that even in this case the presence of confinement could result in various morphologies formed by straight and curved rod-like units.

2. In the presence of a confinement the order parameter $\Phi(\mathbf{r})$ is to be expanded not in the Fourier harmonics, which are the eigenfunctions of the Laplace operator in the

infinite volume, but in the eigenfunctions of the Laplace operator

$$\Delta \Psi(\mathbf{r}) = -E \Psi(\mathbf{r}) \quad (3)$$

for the specified confinement geometry. In the cylindrical co-ordinates, which are the natural choice for ordering in capillaries, the eigenvalues and the corresponding eigenfunctions read

$$E = \alpha_{m,n}^2 + p^2, \quad \Psi(\mathbf{r}) = \sum_{m=-\infty}^{\infty} \sum_{n=1}^{\infty} \int_{-\infty}^{\infty} A_{p,m,n} \exp(ipz) \exp(im\varphi) \phi_{m,n}(r) \frac{dp}{2\pi} \quad (4)$$

Here the order parameter modulations along the cylinder axis and in polar angle are characterized by the wave number p and the integer number m , respectively, whereas $\phi_{m,n}(r)$ are the eigenfunctions of the 2-dimensional radial Laplace operator:

$$\frac{d}{dr} \left(r \frac{d\phi}{dr} \right) - \frac{m^2}{r^2} \phi = -\alpha_{m,n}^2 \phi. \quad (5)$$

$\phi_{m,n}(r)$ are the Bessel functions [25] $J_m(\alpha_{m,n} r)$, the eigenvalues $\alpha_{m,n}^2$ being determined by the corresponding boundary condition. Choosing the reflecting boundary condition

$$\partial \Phi / \partial r|_{r=R} = 0, \quad (6)$$

which is often used to describe the behavior of confined incompressible block copolymer melts [26, 27], we get $\alpha_{m,n}^2 = s_{m,n}^2/R^2$, where $s_{m,n}$ are the locations of extrema of the Bessel function $J_m(x)$ numerated in ascending order.

3. Substituting eqs (4) into (2) we get

$$F_2 = R^2 \int_{-\infty}^{\infty} \sum_{m=-\infty}^{\infty} \sum_{n=1}^{\infty} \Lambda_{m,n}(\tau, p, \rho) \mathcal{N}_{m,n} |A_{p,m,n}|^2 dp, \quad (7)$$

$$\Lambda_{m,n}(\tau, p, \rho) = \tau + (p^2/q_*^2 - \kappa_{m,n}^2)^2, \quad (7)$$

where $\rho = q_* R$ is the reduced capillary radius, $\mathcal{N}_{m,n} = \int_0^1 J_m^2(s_{m,n} x) x dx$ and

$$\kappa_{m,n}^2 = 1 - s_{m,n}^2/\rho^2. \quad (8)$$

The condition providing instability of the disordered state with respect to infinitesimal fluctuations of the (m, n) -mode is

$$\Lambda_{m,n}(\tau, p_{m,n}^*, \rho) < 0, \quad (9)$$

where $p_{m,n}^*$ is location of the absolute minimum of the function (7).

It follows from eqs (7), (8) that the condition (9) takes two rather different forms:

$$p_{m,n}^* = q_* \kappa_{m,n}, \quad \tau < 0, \quad \text{for } s_{m,n} < \rho \quad (10)$$

$$p_{m,n}^* = 0, \quad \tau < -\kappa_{m,n}^4, \quad \text{for } s_{m,n} > \rho. \quad (11)$$



Fig. 1: A typical succession of the ordered (black) and disordered (white) capillary segments for a finite value of the Ginzburg parameter.

In other words, given a finite reduced capillary radius ρ all unstable modes with $s_{m,n} > \rho$ result in an angular and radial modulation only and their contribution to the total order parameter profile is proportional to $J_m(s_{m,n} r/R) \cos(m\varphi)$. On the contrary, the unstable modes with $s_{m,n} < \rho$ possess both an axial and, generally, angular as well as radial modulation.

In the narrow capillaries obeying the inequality

$$\rho < s_{1,1} = 1.841 \quad (12)$$

the only mode (0, 1), which corresponds to the eigenfunction

$$\Phi_{0,1}(\mathbf{r}) = A_0 \cos(q_* z) J_0(s_{01} r/R) = A_0 \cos(q_* z), \quad (13)$$

is axially modulated ($s_{0,1} = 0$). Within the temperature interval ($-\kappa_{1,1} < \tau < 0$) minimizing the free energy (1) we get

$$A_0^2 = -2\tau/3, \quad F_{\text{bulk}} = -T(L/R)\tau^2/\text{Gi}, \quad (14)$$

L and $\text{Gi} = 6v/(\pi R^3)$ being the length of the capillary and Ginzburg parameter, respectively.

4. Indeed, by virtue of the Landau theorem [12], the ordered phase appears as an alternating succession of the ordered and disordered segments of various, generally, lengths (see fig. 1) rather than ordering in the whole capillary. Accordingly, the capillary partition function could be written similarly to that of 1d Ising (helix-coil transition) model [28, 29]:

$$Z(L) = \frac{1}{2\pi i} \int \bar{Z}(p) \exp(pL) dp, \quad (15)$$

where the Laplace transform $\bar{Z}(p)$ reads

$$\bar{Z}(p) = \int_0^\infty \exp(-pL) Z(L) dL = \sigma_i \sigma_j Z_{ij}(p),$$

$$\|Z_{ij}(p)\| = \begin{pmatrix} p & -\sigma \\ -\sigma & p+f \end{pmatrix}^{-1}, \quad (16)$$

where Tf is the specific (per unit length) free energy of the ordered phase, $i, j = 1, 2$ and $\sigma, \sigma_1, \sigma_2$ are, respectively, the weights to be assigned to transient zones between the ordered and disordered segments as well as those between the end-walls of the capillary and the disordered and ordered segments.¹ It follows from eqs (15), (16) that the

¹ Strictly speaking, the free energy $F(l)$ of a capillary segment of the length l is slightly different from fl since for finite segments one should use Fourier series and l -dependent boundary conditions on the end-walls rather than Fourier integrals (5b), which difference is neglected in this paper.

length fraction of the ordered segments is a continuous function of the parameter $u = f/2\sigma$ ($u < 0$ for $\tau < 0$)

$$\phi_{\text{ord}} = -L^{-1} \partial \ln Z(L) / \partial f = (\sqrt{u^2 + 1} - u) / (2\sqrt{u^2 + 1}) \quad (17)$$

Taking into account that $\sigma \sim R^{-1} \exp(fR)$ and, therefore, $|u| \sim |fR| \exp|fR|$, we conclude that capillary ordering is not a genuine phase transition but a co-operative one, the location and width of the transition region being $\tau = 0$ and $|\tau| \sim (\text{Gi})^{1/2}$. Thus, if the inequality (12) holds and $\text{Gi} \ll 1$ then, as is seen from eq (14), for practical purposes the line $\tau = 0$ could be considered as the 2nd order ODT line.

The presented consideration of capillary ordering is extended straightforwardly to the case when the free energy (1) has $N > 1$ minima corresponding to different morphologies, which provides the set f_1, \dots, f_N of the specific (per unit length) free energies. Accordingly, the matrix Z_{ij} and vector σ_i appearing in eq (16) become $N + 1$ -dimensional ones. Then an equilibrium between the segments with different ordered morphologies and the disordered segments would occur, character of which would change on crossover lines. In the limit $\text{Gi} \rightarrow 0$ these crossover lines transform into the 1st order transition lines

$$\min(f_1, \dots, f_N) = f_A = f_B \quad (18)$$

between the ordered morphologies A and B.

5. One more mode, (1, 1), is axially modulated for

$$s_{1,1} < \rho < s_{2,1} = 3.054, \quad (19)$$

two types of the axially modulated profiles being possible:

$$\Phi_{1,1}^{(h)}(\mathbf{r}) = A_h \cos(\varphi \pm p_{1,1} z) J_1(s_{1,1} r/R), \quad (20a)$$

$$\Phi_{1,1}^{(s)}(\mathbf{r}) = A_s \cos(\varphi) \cos(p_{1,1} z) J_1(s_{1,1} r/R). \quad (20b)$$

Further we refer to the profiles (20a) and (20b) as the running along the axes z (helical) and standing waves, respectively. The specific free energies obtained by substituting the order parameter profiles (20) into the free energy (1) read:

$$\tilde{f}_h = \tau \mathcal{N}_{m,n} A_h^2 + (3/4) \mathcal{B}_{m,n} A_h^4, \quad (21a)$$

$$\tilde{f}_s = (\tau/2) \mathcal{N}_{m,n} A_s^2 + (9/32) \mathcal{B}_{m,n} A_s^4, \quad (21b)$$

where $\tilde{f} = fR\text{Gi}$ and $\mathcal{B}_{m,n} = \int_0^1 J_1^4(s_{m,n} x) x dx$, (the difference in the corresponding numerical coefficients is due to difference in averaging the powers of cosines (for F_h) and the products of such powers (for F_s)). Minimizing the free energies (21) with respect to the corresponding amplitudes results finally in the expressions

$$\tilde{f}_h = -2\tau^2 \mathcal{N}_{m,n}^2 \mathcal{B}_{m,n}^{-1}, \quad \tilde{f}_s = -(4/3)\tau^2 \mathcal{N}_{m,n}^2 \mathcal{B}_{m,n}^{-1}. \quad (22)$$

As is seen from (22), the single helical wave is always more thermodynamically advantageous than the standing one

just due to the symmetry properties. The free energies of the left- and right-hand helical waves are identical and the capillary would split into the left- and right-hand helical segments with the average segment length $\sim \sigma^{-2}$ if the helical state is dominant.

For $\rho > s_{2,1}$ at least one more mode (2,1) becomes axially modulated, the contribution of the mode into the total order parameter profile resembles the double (DNA-like) helix:

$$\Phi_{2,1}^{(h)}(\mathbf{r}) = A_{2h} \cos(2\varphi \pm p_{2,1}z) J_2(s_{2,1}r/R) \quad (23)$$

To check whether and when one non-uniform mode gives way to another more thermodynamically advantageous one or a mixture of two modes with further change of the temperature and capillary radius, we substitute into the total free energy (1) a 2-mode trial order parameter profile

$$\begin{aligned} \Phi(r) = & A_1 \mathcal{N}_1 \cos(q_* \kappa_{m_1, n_1} z - m_1 \phi) J_{m_1}(s_{m_1, n_1} r/R) \\ & + A_2 \mathcal{N}_2 \cos(q_* \kappa_{m_2, n_2} z - m_2 \phi) J_{m_2}(s_{m_2, n_2} r/R) \end{aligned} \quad (24)$$

The proper choice of the normalizations \mathcal{N}_i leads to the reduced specific free energy

$$\begin{aligned} \tilde{f} = 3 \min F(A_1, A_2), \quad F(A_1, A_2) = & \tau_1 A_1^2 + \tau_2 A_2^2 \\ & + (3/8)(C_1 c_{11} A_1^4 + 2c_{12} A_1^2 A_2^2 + C_2 c_{22} A_2^4), \end{aligned} \quad (25)$$

where $c_{ij} = 2 \int_0^1 J_{m_i}^2(s_{m_i, n_i} x) J_{m_j}^2(s_{m_j, n_j} x) x dx / \mathcal{N}_i \mathcal{N}_j$, $c_{ii} = \int_0^1 J_{m_i}^4(s_{m_i, n_i} x) x dx / \mathcal{N}_i^2$, $\tau_i = \tau + \kappa_{m_i, n_i}^4$ for the modes (10) and $\tau_i = \tau$ for the modes (11), $C_i = 2/3$ if the i -th mode is a mode (0, n) belonging to the type (10) and $C_i = 1$ otherwise.

The straightforward analysis shows that the minimum of the free energy (25) is achieved in a 1-mode state only ($A_1 = 0$ or $A_2 = 0$) if the determinant $|c_{ij}|$ is negative, the transition between the modes being the discrete 1st order phase transition in the limit $\mathbf{G}i \rightarrow 0$. If $|c_{ij}| > 0$ then the minimum of the free energy (25) could correspond to a 2-mode state ($A_1 \neq 0$ and $A_2 \neq 0$), the second mode appearing (in this limit) via the continuous 2nd order phase transition.

The corresponding calculations are straightforward for the reflecting boundary condition (6). Somewhat unexpectedly from the mathematical standpoint there is only one dominant mode (0, 1), which corresponds to the order parameter profile $\Phi(r) = A \exp(iq_* z)$. All other modes, even those unstable being single, are suppressed in the presence of this dominant mode. But from the physical viewpoint it is quite natural. Indeed, the boundary condition (6) does not change the ordering conditions as compared to that in bulk, where the lamellar morphology is the most stable one. Thus, any other ordered morphology would cause only some additional frustration without any compensation.

6. The situation changes drastically if there is a preferential adsorption of the system particles to the boundary,

which is naturally described by an additional linear surface term [30]:

$$F = F_{\text{bulk}} + F_{\text{surf}}, \quad F_{\text{surf}} = (hT/v) \int \Phi(\mathbf{r}) dS, \quad (26)$$

h being the strength of the preferential adsorption. Obviously, the term (26) affects the modes (0, n) with n high enough to be of the type (11) and thus favors the coaxial morphologies. Say, the mode (0, 2) is dominant in the narrow capillaries satisfying the inequality

$$\rho < s_{0,2} = 3.832 \quad (27)$$

if $|\tau|$ is not too big. If $\tau \rightarrow -\infty$ the mode (0, 1) becomes dominant since it has the smallest quantitative value of the reduced forth vertex. To find the 1st order transition line (18) between the modes (0, 1) and (0, 2), it is convenient to rewrite eq (25) in the reduced variables $A = H^{1/3} B$, $\tau = H^{2/3} t$, $H^{4/3} \tilde{f} = 3 \min F(B_1, B_2)$:

$$\begin{aligned} F(B_1, B_2) = & b B + t_1 B_1^2 + t_2 B_2^2 \\ & + (3/4) B_1^4 + 3 B_1^2 B_2^2 + (c_{22}/4) B_2^4. \end{aligned} \quad (28)$$

The fields B_1, B_2 correspond to the modes (0, 1), (0, 2), $b = 6J_0(s_{0,2})/(\mathcal{N}_{0,2})^{1/2}$, $\tilde{\tau}_2 = \tilde{\tau} + \kappa_{0,2}/h^{2/3}$ and $H = h/R$.

In fact, however, the transition found by minimization of the function (28) turns out to be only metastable. The case is that, contrary to the slab mode (0, 1), the coaxial mode (0, 2) could be compatible (form a mixed state) with some helical or angular modes, in particular, simple helix (1, 1), double helix (2, 1), (3, 1), (3, 2), (4, 1), (4, 2) and so on. Thus, to build the phase diagram we are to analyze, which of the pure or mixed modes is the most thermodynamically favorable and in which temperature interval. In fact, it is sufficient to take into account only the modes $\{(1, 1), (2, 1)\}$, which would start to grow early than the coaxial mode (0, 2) in the absence of any preferential adsorption. The resulting phase diagrams within the interval (27) are shown in fig. 2. Remember that in the regions 2b, 3b the long segments with the left-hand helical waves alternate with the right-hand ones since the free energies of both are identical.

It is easy to see that increase of the surface field h results in increase of the temperature width $\Delta\tau$ ($\Delta\tau \sim 10 h^{2/3}$) of the region, where the helical ordering can be observed. Besides, the regions of purely angular ordering 2a and 3a, which are just negligible for small h , grow considerably with increase of h . It is convenient to visualize the character of the appearing angular and/or helical ordering by the curves $r(\phi)$ satisfying equation

$$\Phi(r, \phi) = 0, \quad (29)$$

where the order parameter $\Phi(\mathbf{r})$ is given by expression (24) with $m_1 = 0, n_1 = 2$ and $m_2 = 1(2), n_2 = 1$. The curves (29), which could be considered as intersections of the conditional interfaces between the domains with the

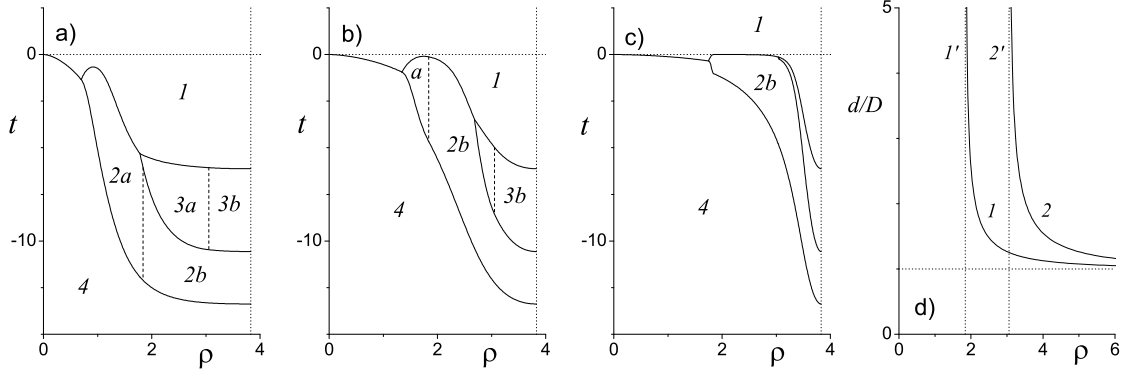


Fig. 2: The reduced phase diagrams of ordering in the most narrow capillaries satisfying condition (27) for $h = 100$ (a), $h = 1$ (b) and $h = 0.01$ (c) as well as (d) the dependences of the pitches d (normalized on the lamellar period in bulk D) of the ordinary (1) and double (2) helices on the reduced capillary radius ρ . The regions 1 and 4 correspond to the coaxial (0, 2) and slab (0, 1) modes, the regions 2 and 3 do to the mixed (0, 2) + (1, 1) and (0, 2) + (2, 1) states, respectively. The dotted horizontal and vertical lines on figures (a)-(c) correspond to the bulk ODT temperature $\tau = 0$ and the boundary (27), respectively. The dotted vertical lines 1' and 2' on figure (d) are the asymptotes $\rho = s_{1,1}$ and $\rho = s_{2,1}$ of the curves 1 and 2, they correspond to the dashed vertical lines on figures (a)-(c) separating the regions a and b of the axially non-modulated and modulated states of the same modes. The dotted horizontal line $d = D$ on figure (d) is the common asymptote of the curves 1 and 2 at $\rho \rightarrow \infty$.

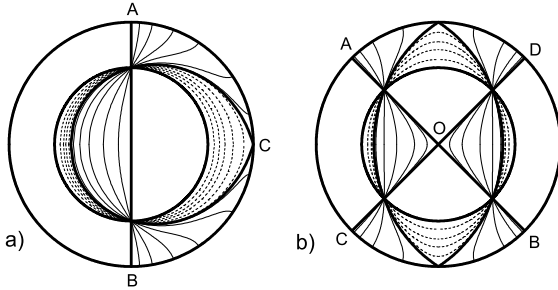


Fig. 3: The curves (29) (domain interfaces) in the 1-thread helix (0, 2)+(1, 1) and double DNA-like helix (0, 2)+(2, 1). The outer bold circle is the capillary cross-section, the inner one is the interface for the pure (0, 2) mode ($x = \infty$). With decrease of x the 1-thread helix interface (a) becomes more and more eccentric (the plotted dashed curves correspond consecutively to $x = 5, 3, 2.25, 1.75, 1.5$) until the interface (bold solid curve) touches the capillary wall at $x = 1.445$. Next the contact area extends (see the thin solid curves corresponding to $x = 1.4, 1.2, 0.8, 0.5, 0.25, 0.1$) and at $x = 0$ the interface is just the diameter AB. The double helix interface (b) undergoes a similar evolution but the fact that it is centrosymmetrical.

cross-sections normal to the capillary axes, are plotted in fig. 3 for various values of the ratio $x = A_1/A_2$, where A_i are the coefficients appearing in the expression (24).

Beyond the interval (27) the mode (0, 2) is axially modulated and does not contribute into the surface term (26)

anymore. If $|\tau|$ is not too big, then the modes (0, n) are dominant within the intervals $s_{0,n-1} < \rho < s_{0,n}$. With the temperature decrease the pure coaxial modes are subsequently replaced by their various combination with the compatible helical or angular modes until the slab mode (0, 1) wins finally for $\tau \rightarrow -\infty$. Thereby, the sets of relevant compatible modes are fast growing with increase of the reduced capillary radius ρ and, thus, n , which makes calculation of the dominance maps rather cumbersome. E.g., the relevant sets are $\{(1, 1), (2, 1), (3, 1), (4, 1)\}$ for $n = 3$ and $\{(1, 1), (2, 1), (3, 1), (4, 1), (3, 2), (4, 2)\}$ for $n = 4$ (other modes with $s_{m,n} < s_{0,3(4)}$ are incompatible with the corresponding coaxial modes). The occurring morphologies appear as ordinary, double (DNA-like) or multi-helix structures (sometimes coaxial ones with the same pitch) entwining central straight rod. These morphologies resemble those seen under simulation of the asymmetric (with non-zero cubic term) block copolymers in refs [1,9] and are rather different from the lamellar morphology to be observed in the bulk for the case considered here ($\alpha = 0$).

Summarizing, we have shown that emergence of various helical and other complex morphologies in systems undergoing ordering when they are confined to cylindrical geometry is a rather general result of interplay between the geometrical and energetic effects of confinement even in the seemingly trivial case of the reflecting boundary condition (6) and zero cubic term. For this case a detailed "dominance map" (in the limit $Gi \rightarrow 0$ it is just the phase diagram) including various complex structures,

is presented.

The actual phase diagram of particular real systems could differ from that build in fig. 2. First, the cubic term, if present, would contribute to stability of the found morphologies formed by straight and curved rod-like units. Next, the numerical values of the effective fourth vertices c_{ij} , which appear in the 2-amplitude Landau expansion (25) and determine eventually the shape of the phase diagrams shown in fig. 2, depend on the assumption of locality of the fourth vertex in the Landau Hamiltonian (1) used in this paper. If the vertex is non-local and reads $\int \Gamma(\mathbf{r}_1, \mathbf{r}_2, \mathbf{r}_3, \mathbf{r}_4) \prod_{i=1}^4 \Phi(\mathbf{r}_i) d\mathbf{r}_i$, then an "angle dependence" [14, 31, 32] of the fourth vertex appears. When strong enough, the dependence is known to change the sequence of the stable morphologies even in bulk [31–33]. Thus, it could change the phase diagram shown in fig. 2 either.

Our results suggest also that it could be fruitful to analyze experimental or numerical data in terms of Bessel functions or of their underlying symmetry. More detailed presentation of the Landau theory including discussion of other possible boundary conditions and microscopic theory of block copolymer will be given in an extended version of this paper.

* * *

The authors thank the program ENS-Landau for financial support of this work.

REFERENCES

- [1] WU Y., CHENG G., KATSOV K, SIDES S.W., WANG J., TANG J., FREDRICKSON G.H., MOSCOVITS M. and STUCKY G.D., *Nature Materials*, **3** (2004) 816.
- [2] SHIN K., XIANG H., MOON S.I., KIM T., MCCARTHY T.J. and RUSSELL T.P., *Science*, **306** (2004) 76.
- [3] XIANG H., SHIN K., KIM T., MOON S.I., MCCARTHY T.J. and RUSSELL T.P., *Macromolecules*, **37** (2004) 5660.
- [4] XIANG H., SHIN K., KIM T., MOON S.I., MCCARTHY T.J. and RUSSELL T.P., *Macromolecules*, **38** (2005) 1055.
- [5] XIANG H., SHIN K., KIM T., MOON S.I., MCCARTHY T.J. and RUSSELL T.P., *Journal of Polymer Science: Part B: Polymer Physics*, **43** (2005) 3377.
- [6] YIMING SUN, MARTIN STEINHART, DANILO ZSCHECH, RAMESHWAR ADHIKARI, GOERG H. MICHLER and ULRICH GOSELE, *Macromol. Rapid Commun.*, **26** (2005) 369.
- [7] HE X., SONG M., LIANG H. and PAN C., *J. Chem. Phys.*, **114** (2001) 10510.
- [8] FENG, J. and RUCKENSTEIN, E., *Macromolecules*, **39** (2006) 4899.
- [9] BIN YU, PINGCHUAN SUN, TIEHONG CHEN, QINGHUA JIN, DATONG DING, BAOHUI LI and AN-CHANG SHI, *Phys. Rev. Lett.*, **96** (2006) 138306.
- [10] SEVINK G.J.A., ZVELINDOVSKY A.V., J. G. E. M. FRAALJE H. and HUININK P., *J. Chem. Phys.*, **115** (2001) 8226.
- [11] LI W., WICKHAM R.A. and GARBARY R.A., *Macromolecules*, **39** (2006) 806.
- [12] LANDAU L.D. and LIFSHITZ E.M., *Statistical Physics, Part 1* Pergamon Press 1980.
- [13] DE GENNES P.G., *Faraday Disc. Chem. Soc.*, **68** (1979) 96.
- [14] LEIBLER L., *Macromolecules*, **13** (1980) 1602.
- [15] ERUKHIMOVICH I. YA., *Polymer Sci. U.S.S.R.*, **24** (1982) 2223, 2232.
- [16] LANDAU L. D., *Phys. Zs. Sowjet*, **11** (1937) 545.
- [17] KATS E.I., LEBEDEV V.V. and MURATOV A.R., *Phys. Rep.*, **228** (1993) 1.
- [18] BRAZOVSKII S.A. and DMITRIEV S.G., *Sov. Phys. JETP*, **42** (1975) 497.
- [19] WRIGHT D.C. and MERMIN N.D., *Rev. Mod. Phys.*, **61** (1989) 385
- [20] NABUTOVSKII V.M., NEMOV N.A. and PEISAKHOVICH YU.G., *Sov. Phys. JETP*, **52** (1980) 1111.
- [21] HØYE J. S. and STELL G., *J. Phys. Chem.*, **94** (1990) 7899.
- [22] BORUE V.YU. and ERUKHIMOVICH I.YA., *Macromolecules*, **21** (1988) 3240.
- [23] JOANNY J.-F. and LEIBLER L., *J. Phys. (Paris)*, **51** (1990) 545.
- [24] CIACH A. and BABIN V., *J.Mol.Liq.*, **112** (2004) 37.
- [25] BATEMAN H. and ERDELYI A., *Higher Transcendental Functions*, Vol. **2** Mc Graw-Hill Book Company, inc., New York Toronto London 1953
- [26] ANGERMAN H.J., JOHNER A. and SEMENOV A.N., *Macromolecules*, **39** 2006 6210.
- [27] STEPANOW S. and FEDORENKO A.A., *Phys. Rev. E*, **73** 2006 031801.
- [28] KERSON HUANG, *Statistical Mechanics* John Wiley and Sons, Inc., New York -London 1994
- [29] GROSBURG A.YU. and KHOKHLOV A.R., *Statistical Physics of Macromolecules* American Insitute of Physics, NY, 1994
- [30] FREDRICKSON G.H., *Macromolecules*, **20** (1987) 2535.
- [31] ERUKHIMOVICH I.YA., *JETP Lett.*, **63** 1996 459.
- [32] ERUKHIMOVICH I.YA., *Eur. Phys. J. E*, **18** 2005 383.
- [33] SMIRNOVA YU.G., G. TEN BRINKE and ERUKHIMOVICH I.YA., *J. Chem. Phys.*, **124** 2006 054907.